Int. J. Electrochem. Sci., 9 **(2014)** 2848 - 2858

International Journal of
ELECTROCHEMICAL
SCIENCE
www.electrochemsci.org

Toughness of SAE 1020 Steel with and without Galvanization Exposed to Different Corrosive Environments in Chile

Paula Rojas[1], *Carola Martínez*[1], *Rosa Vera*[2], *Mónica Puentes*[2]

[1] Escuela de Ingeniería Mecánica, Facultad de Ingeniería, Pontificia Universidad Católica de Valparaíso, Los Carrera 01567, Casilla 4059, Quilpué, Chile.
[2] Instituto de Química, Facultad de Ciencias, Pontificia Universidad Católica de Valparaíso, Av. Universidad 330, Casilla 4059, Curauma, Valparaíso, Chile.
*E-mail: paula.rojas.s@ucv.cl

Received: 28 October 2013 / *Accepted:* 6 December 2013 / *Published:* 23 March 2014

In this study, SAE 1020 steel Charpy´s samples, with and without galvanization, were exposed to a large variety of environmental conditions throughout Chile in order to ascertain the degree of deterioration due to environmental corrosion. The levels of Cl^-, SO_2 and time of wetness were also registered in order to be able to correlate the data with respect to corrosion rate with the environmental and meteorological parameters. Calculations of corrosion rates were made via loss of weight and analysis of surface deterioration using scanning electron microscopy. After different exposure periods up to 33 months, the samples were tested and analyzed. According to the results, the toughness of the steel without galvanization can vary from 70 to 10 J; this variation reveals a dramatic change of property that is as much a function of the different atmospheres as of the exposure time. In comparison to the non-galvanized steel, the galvanized has a lower initial toughness, but it remains more constant over time, maintaining a range of 20 to 7 J.

Keywords: Toughness, Atmospheric Corrosion, Galvanized Steels.

1. INTRODUCTION

Atmospheric corrosion is a worrying issue across the world due to its importance in the useful life of structural materials. The economy of countries would change drastically if there were no corrosion. Atmospheric corrosion, compared to other types of corrosion, leads to the highest amount of loss and is most significant in areas where the level of aggressiveness of the environment is high [1]. Conventional atmospheric parameters that can lead to metal corrosion are factors such as temperature,

humidity, precipitation, solar radiation, wind speed, etc. Another important factor is air pollutants such as sulfur or carbon dioxide, chlorides, hydrogen sulfide, nitrogen oxides, etc. [2].

Atmospheric corrosion of steel has been studied by many authors, focusing on aspects such as reactions, layers and corrosion products [3-9]. However, evaluation of damaged caused by the phenomenon on the properties of the material has not seen widespread study, particularly when the forces applied are not tensile.

When evaluating the mechanical properties of different steels exposed to atmospheric corrosion, there is documentation on how tensile strength drops as a function of different atmospheres and exposure times [10, 11], where the fall in mechanical strength (YS and UTS) is attributed to heterogeneously distributed corrosion products on the material surface, leading to surface roughness and increasing the possibility of force concentration and/or localized corrosion [12]. M. Okayasu et al. [13] show that fatigue strength is directly affected by surface morphology; the rougher the surface, the lower the fatigue strength. This was similarly shown by Suresh [14], stating that the formation of pitting on initially smooth surfaces produces a significant reduction in fatigue strength. Ragah et al. [15] used Izod impact testing to find that when subjecting 3 types of steel to different corrosion environments, impact resistance falls as a function of the aggressiveness of the corrosive environment and of the characteristics of the steel.

In terms of fracture toughness, steel is a family of alloys that present very varied behavior. The reason for these differences is that the toughness of the steel is affected not only by its composition, but also by changes in microstructure [16, 17] and the temperature at which the test is carried out [18].

The toughness values of carbon steels can vary from 10 to 200 J, depending on carbon content [19] and testing temperature. However, at the same time, for materials that have been formed previously with a microstructure that is anisotropic, a phenomenon known as toughness anisotropy is seen, where the value can vary up to 20 J, depending on the direction in which the test is conducted [20].

In general, when a high level of toughness is required for an application of low-alloy carbon steel, it is recommended that the carbon content, the grain size and the non-metallic inclusions are minimized. Although toughness values for steel and other metallic materials are relatively easy to determine though mechanical testing, there is little documentation on the possible effect of corrosion on these materials or on how protection systems against corrosion can also affect this property.

The Charpy impact test has been used to evaluate the toughness of metallic materials for a hundred years; it is a standardized test and is used widely in industry due to its simplicity, speed and low cost. In this study it is used to compile values on different samples of SAE 1020 steel with and without galvanization, exposed at stations with different climatic conditions distributed throughout Chile, over a maximum exposure period of 33 months.

2. EXPERIMENTAL PART

The studied material is a SAE 1020 steel with and without galvanization; the chemical compositions were analyzed by X-ray Spectrometry and listed in Table 1.

Table 1. Chemical composition of tested steels

	C	Mn	P	S	Si	Cr	Ni	Mo	Cu	V	Ti	W	Zn	Al
Steel	0.098	0.28	0.012	0.015	0.15	0.03	0.04	0.07	0.03	<0.01	<0.01	<0.01	-	-
Galv.	-	-	-	-	-	-	-	-	-	-	-	-	98.5	0.5

*Fe balance.

Standard Charpy specimens measuring 55 mm x 2 mm x 2 mm composed of SAE 1020 steel with and without galvanization were installed at 21 study stations throughout Chile (see Figure 1) from March 2010 for a period of 33 months. In order to simultaneously monitor the effect of atmospheric corrosion on toughness, 100 mm x 100 mm x 4 mm specimens were also installed at an angle of 45° and separated by plastic barriers in accordance with ISO Standards 9223 to 9226 [21-24].

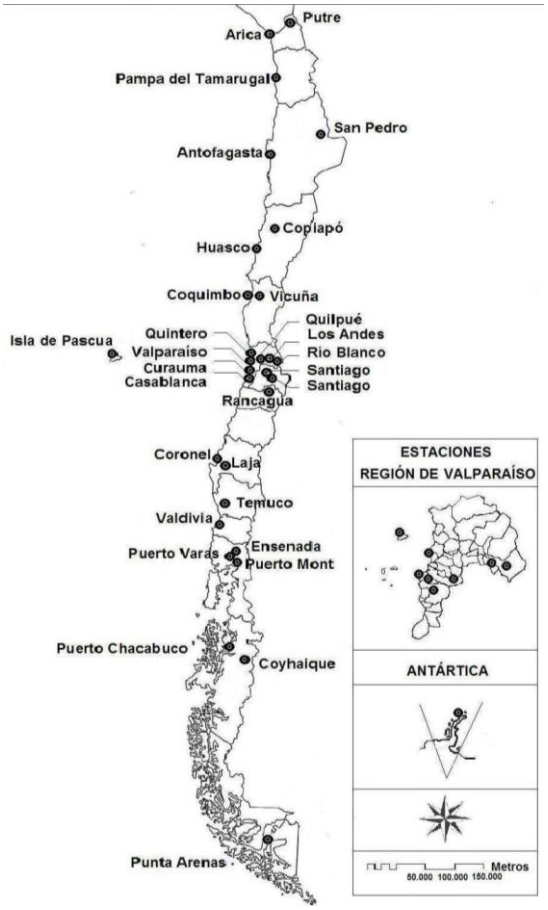

Figure 1. Location of the corrosion testing stations in Chile.

Devices were installed at each station to take bimonthly readings of atmospheric chloride and sulfur dioxide content, along with weather stations to obtain data on temperature, atmospheric humidity, rainfall and wind speed and direction, at the sites where this information was not available. The data on temperature and relative humidity was used to determine time of wetness (TOW) on a monthly basis.

The corrosion products were studied by X-ray diffraction (XRD) in a SIEMENS D-5000 diffractometer using Cu-Kα radiation. The corrosive deterioration of the materials was evaluated every 3 months by measuring the mass loss in triplicate (ASTM G50 [25]) and the morphology of the metal attack was evaluated using scanning electron microscopy (SEM) with a JEOL 5410 microscope coupled to a EDAX 9100 analyzer for element characterization.

The toughness tests were carried out with a JB-S300 Instrumented Charpy Impact Testing Machine, with a capacity of 300 J and digital data readout.

3. RESULTS AND DISCUSSION

3.1. Corrosion of SAE 1020 Steel with and without Galvanization

Figure 2 shows the corrosion rates of the carbon steel measured at each station up to 15 months of exposure (Figure 2a) and up to 30 months exposure (Figure 2b). In general, it can be seen that the corrosion rate decreases with increased exposure time at each station.

The stations with highest rates of corrosion are located in Quintero, Coronel, Antarctica, Arica, Easter Island and Huasco. At the remaining stations, the corrosion rate is less than or equal to 50 µm/year at 12 months and 12 µm/year at around 30 months. It is important to note that at most of the stations the corrosion rate value at 3 months is higher due to the kinetics of the process, which is associated with the capacity to form corrosion products and their protective nature [26].

X-ray diffraction was used to identify the corrosion products at 12 months exposure, showing that the steel corrodes to form iron oxide at all the stations. However, at the Laja station, which presents a low corrosion rate, there is presence of SiO_2 from the soil, while at Quintero there is FeS, as the station has high SO_2 content. At the Arica and Easter Island stations, the presence of oxide-hydroxide mixtures is seen on the steel as these stations are located close to the coastline (see Figure 3).

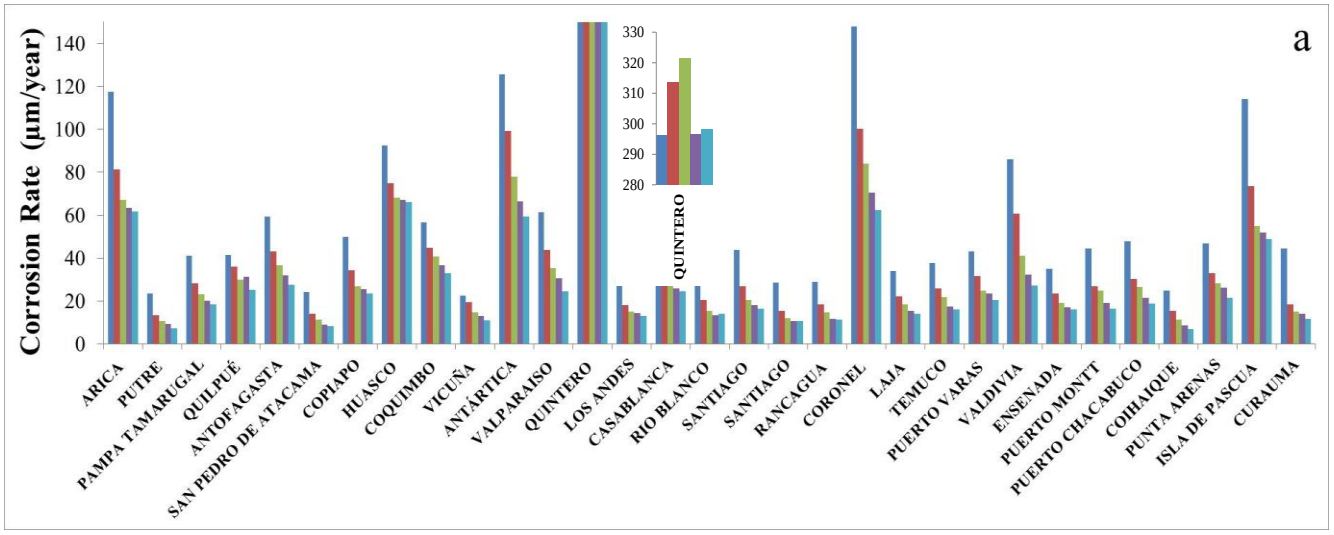

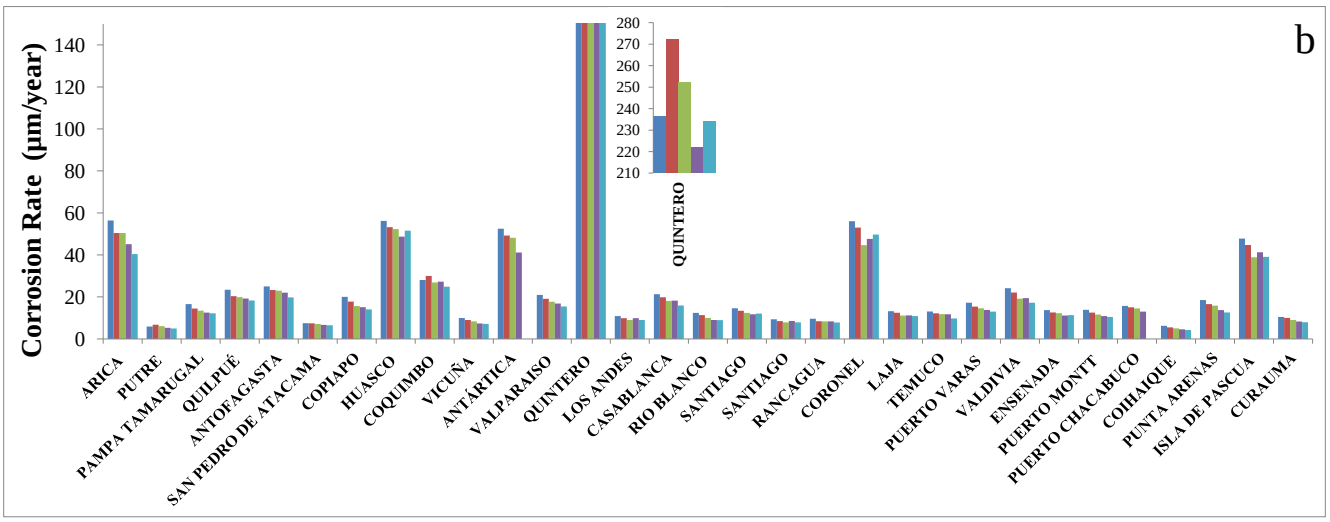

Figure 2. Corrosion rate of SAE 1020 carbon steel after a) 3, 6, 9, 12 and 15 and b) 18, 21, 24, 27 and 30 months exposure.

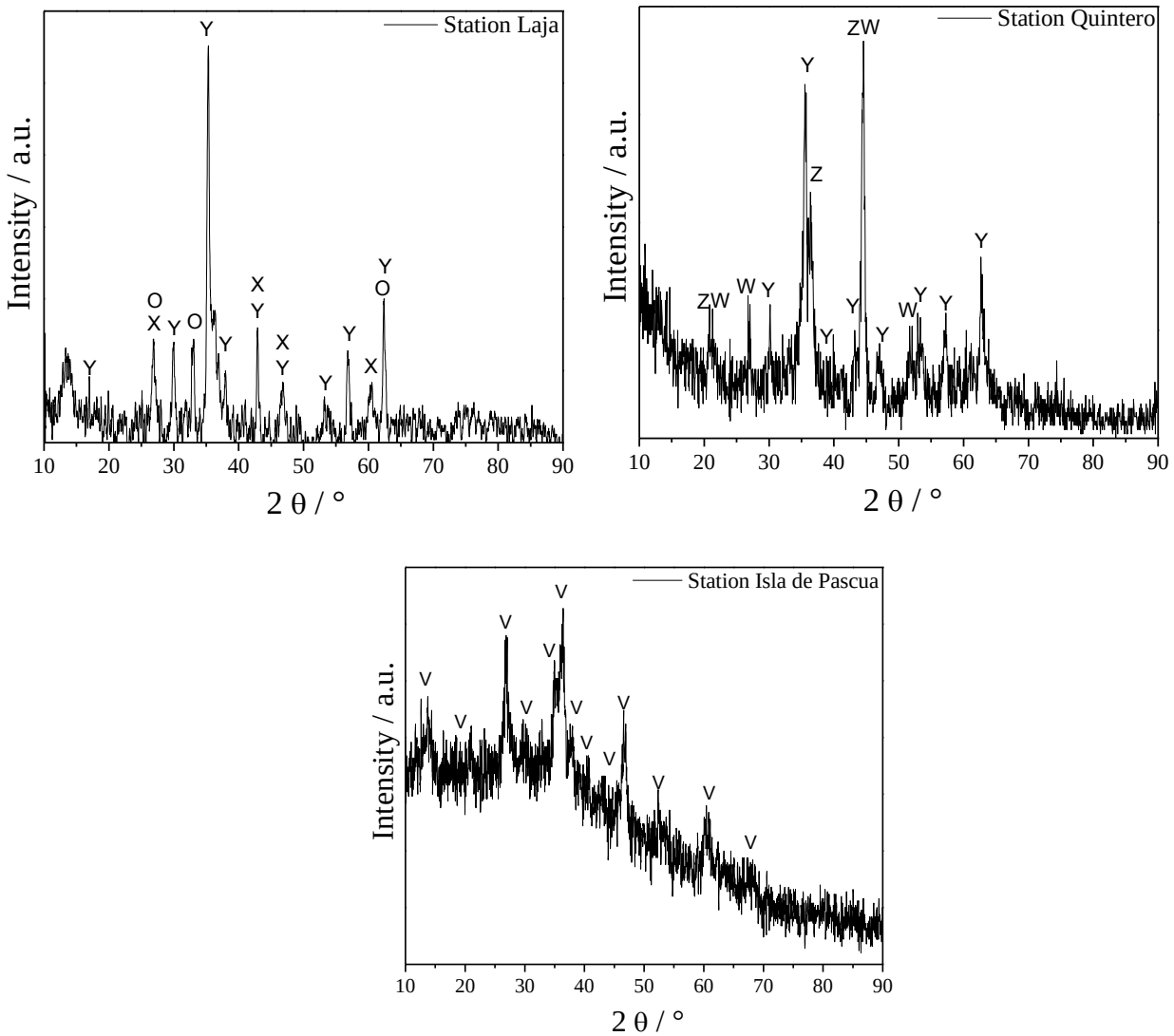

Figure 3. XRD pattern of the corrosion products on the steel at 12 months. (x=SiO_2, o=Si, y=Fe_3O_4, z= Fe_2O_3, w=FeS, v= FeOOH).

Figure 4 shows the corrosion rates for galvanized SAE 1020 steel, measured at each station throughout Chile. Figure 4a shows the results up to 15 months exposure and figure 4b shows up to 30 months exposure. It can be seen that the corrosion rate is much lower, with an average of 2 µm/year, except at the stations with higher corrosion rate, which are Arica, reaching a maximum of 12 µm/year at 9 months, Quintero, with a maximum of 16 µm/year at 15 months, and also Easter Island and Huasco to a lesser extent.

This therefore proves that the protection given by galvanization is effective in reducing corrosion rate [27].

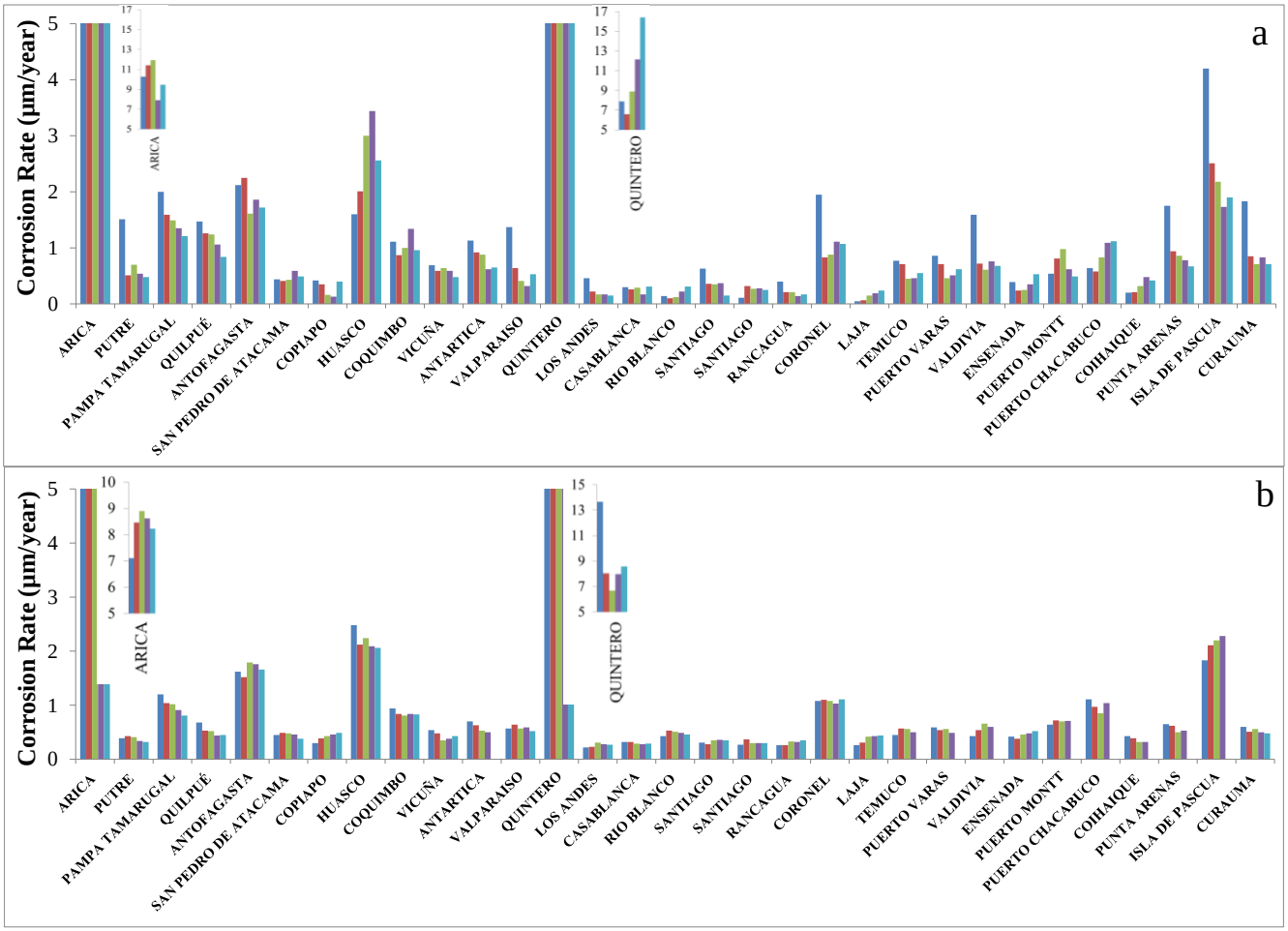

Figure 4. Corrosion rate of galvanized SAE 1020 carbon steel after a) 3, 6, 9, 12 and 15 and b) 18, 21, 24, 27 and 30 months exposure.

Scanning electron microscopy was used to determine the morphology of the corrosion products at the different stations. Figure 5 shows the micrographs of the carbon steel after 12 months exposure at the Huasco station (Figure 5a) and Antarctica (Figure 5b), which showed similar corrosion rate behavior. A larger amount of corrosion product can be seen on the Huasco sample, while the layers of corrosion product on the Antarctica specimen are flat and compact, though fissures are visible, thus allowing the metal-corrosion product interface to remain active in the saline atmosphere. As both

stations are close to the sea, increasing the deterioration of the material, a similar morphology is to be expected in the corrosion products. However, the differences in temperature, humidity, wind and snow found at the Antarctica station lead to a notable change in the morphology of the corrosion products.

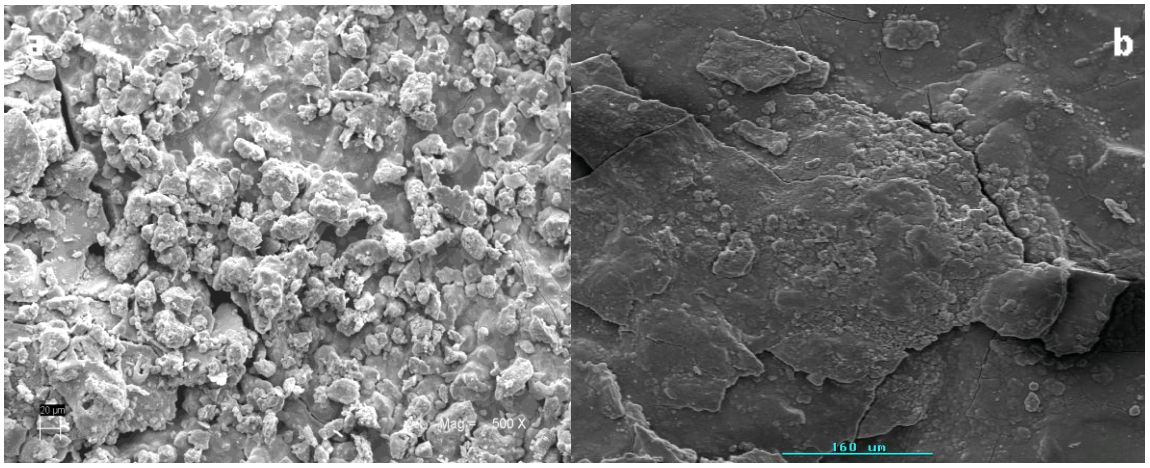

Figure 5. Micrographs of the carbon steel after one year of exposure at the a) Huasco and b) Antarctica stations. 500x

Figure 6 shows the morphology of the corrosion products on galvanized steel at (a) Quintero and (b) Easter Island, after one year of exposure. It is evident that a large amount of grainy and distributed corrosion product forms across the surface of the Quintero specimen, while the corrosion product on the Easter Island sample is much smaller in size and presents flat areas.

This behavior was to be expected, as the Quintero area shows the highest corrosion rate (12 µm/year) while at the Easter Island station the corrosion rate is approximately 2 µm/year, which is in line with the amount of corrosion product formed.

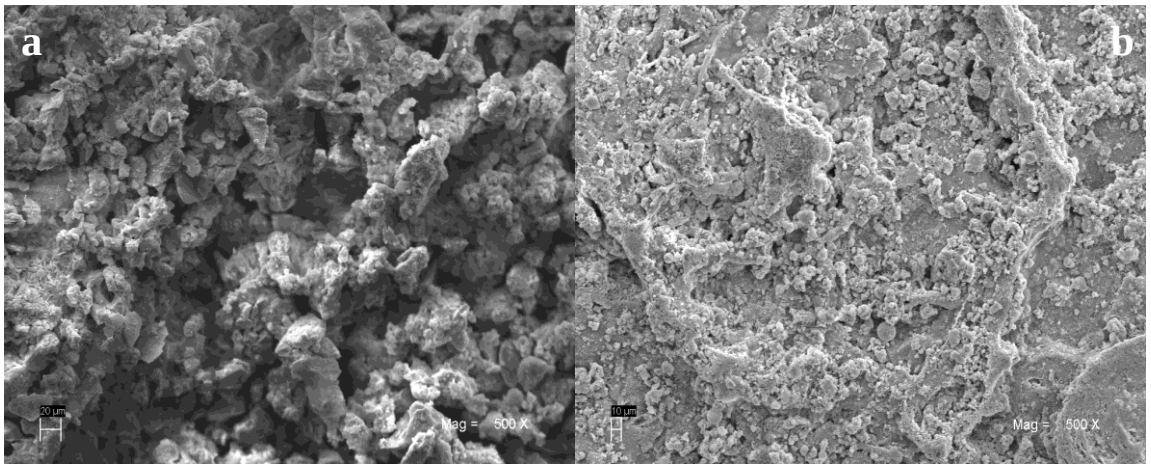

Figure 6. Micrographs of galvanized steel after one year of exposure at the (a) Quintero and (b) Easter Island stations. 500x

3.2. Fracture Toughness of the SAE 1020 Steel with and without Galvanization

Figure 7 shows micrographs of the surface and cross-section of the galvanized SAE 1020 steel specimen. The layer of η-Zn (100% Zn) has an approximate thickness of 30 µm, the other layers that can be seen are a ζ phase ($FeZn_{13}$) with a thickness of 80 µm and a composition of 93.1% Zn and 6.9% Fe, identified by EDAX; δ-Zn (~90% Zn), though the phases such as δ_1 ($FeZn_7$), Γ_1 (Fe_5Zn_{21}) and Γ (Fe_3Zn_{10}) could not be clearly distinguished; and the lower part of the cross-section is γ-Zn (~75% Zn) followed by the final steel matrix.

The fracture toughness values of the SAE 1020 steel samples with and without galvanization without exposure to corrosive media were 32 J and 13 J, respectively. The galvanized steel has different layers of Zn (see figure 7) whose toughness is lower compared to the pure iron.

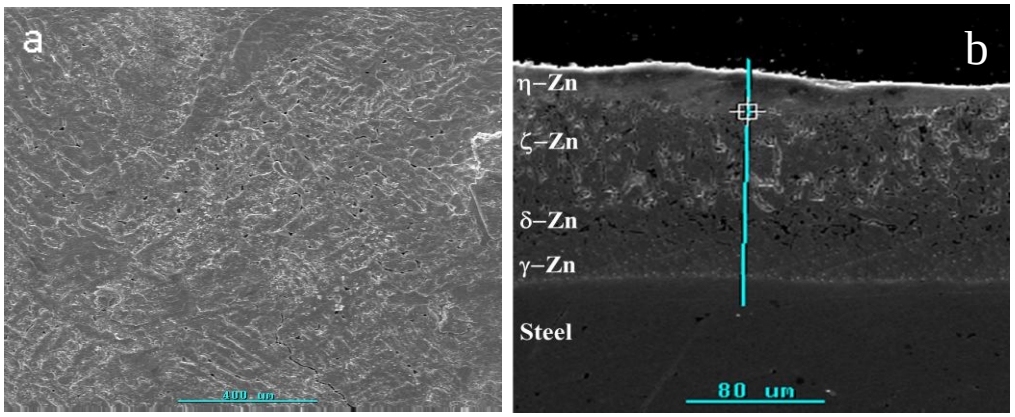

Figure 7. Metallographs of the hot-dip galvanized SAE steel a) Surface appearance and b) Cross section.

From the figures for toughness measured after 3 months exposure shown in Figure 8, it can be seen that there is variation in toughness between different specimens from the same station.

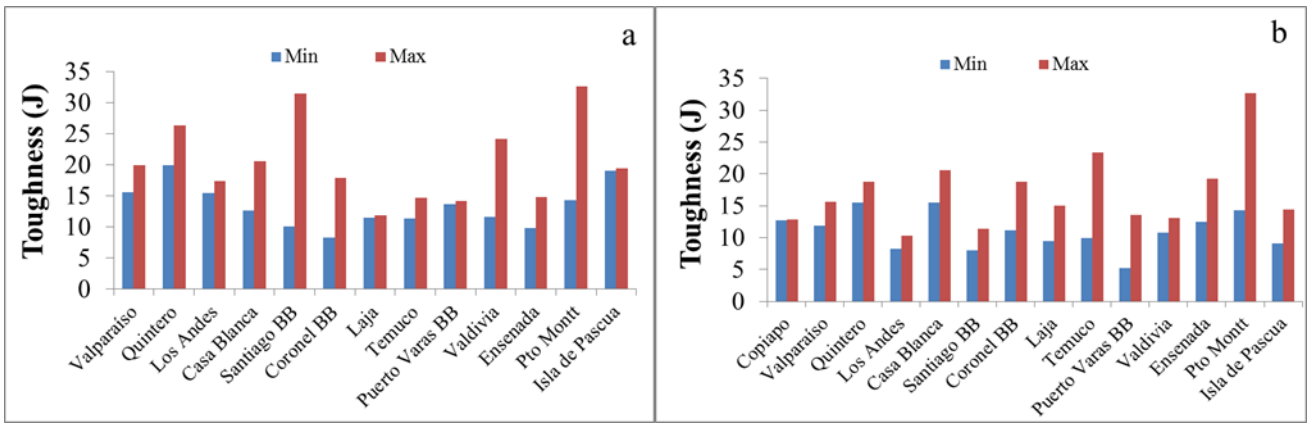

Figure 8. Variation in toughness of samples of a) SAE 1020 steel and b) galvanized SAE 1020 steel after 3 months exposure.

Figure 9 shows photographs of two specimens hung up for exposure at the station located in Quilpue after 12 months exposure. As can be seen in figures 9a and 9b, some specimens show a large degree of corrosion in the slit, while this is not seen on other specimens, which leads to widely dispersed results. This difference in behavior in the specimen's slit is attributed to deviation in the relative angle of the specimens due to environmental variations, either wind, rain, etc., as seen in Figure 9c. Vera et al. [28] showed the influence of exposure angle on corrosion behavior, also considering that the connection between electrolyte-material depends on contact time, i.e. the time that the electrolyte remains in the slit, and this in turn is influenced by the angle of inclination of the specimen.

Regarding the toughness behavior of the SAE 1020 steel as a function of exposure time, figure 10 shows comparative values for toughness after 3, 21 and 33 months exposure at some of the study stations. Comparing the different exposure times (Figure 10) it can be seen that in some cases, particularly in rainy areas, the toughness of the SAE 1020 steel fell to the level of the galvanized material itself and even lower. This shows that a material that is initially tough can lose this property as a result of atmospheric corrosion. At the Laja station, looking at the non-galvanized steel, the corrosion rate decreases with increased exposure time, which can also be seen in the increase in toughness value, possibly due to the existence of more homogenous corrosion products.

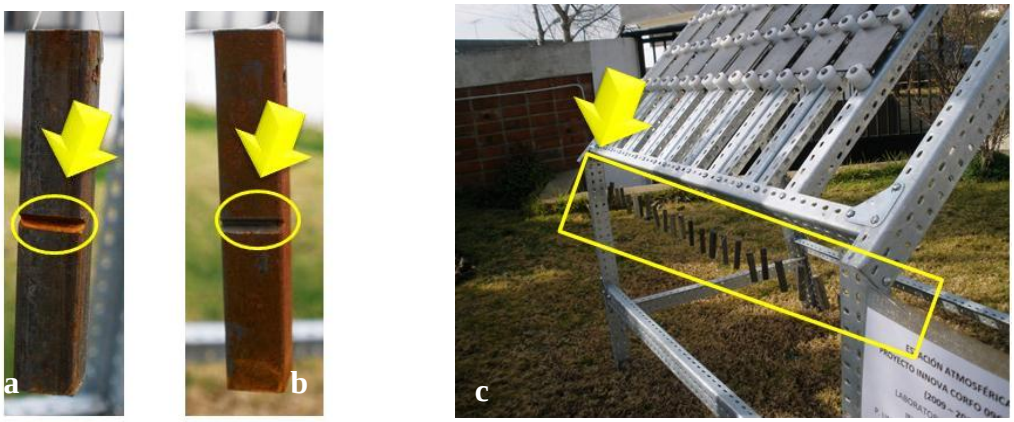

Figure 9. SAE 1020 steel specimens after 12 months exposure (a) sample with heavily corroded slit, (b) slit with homogenous corrosion and c) support structure with SAE 1020 steel specimens.

The layers formed during the hot-dip galvanization process give the galvanized steel a very different microstructure to that of the non-galvanized steel (Figure 7). These layers protect the steel from corrosion, but decrease toughness, though the latter value is more stable over time than with the non-galvanized steel.

Therefore, it can be seen that damage caused by atmospheric corrosion of steel also affects the fracture toughness of the SAE 1020 steel, where the corrosion produces a decrease in toughness to a lower level than that of the galvanized material and which becomes less stable over time.

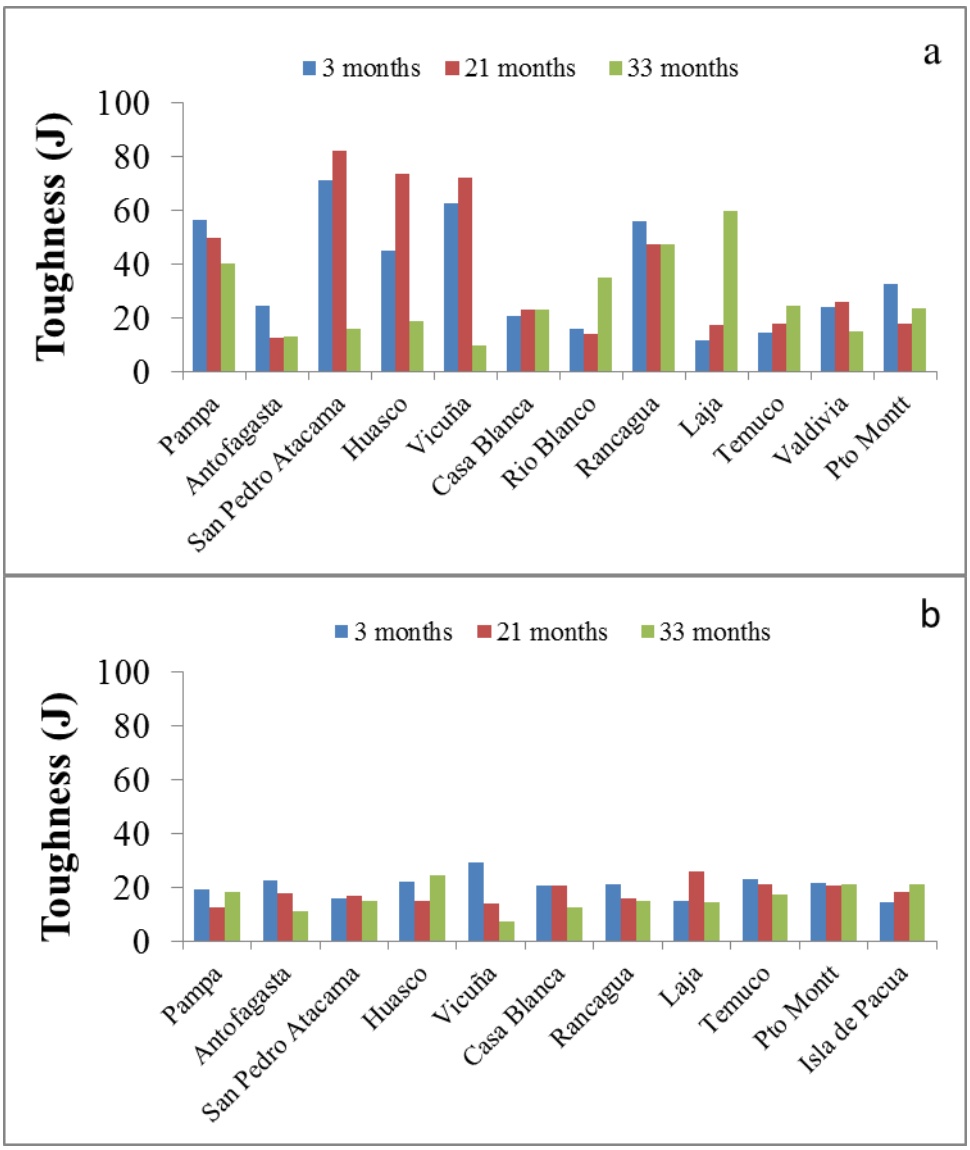

Figure 10. Variation in the toughness of the samples of a) SAE 1020 steel and b) galvanized SAE 1020 steel as a function of exposure time (3, 21 and 33 months)

4. CONCLUSIONS

The main conclusions from the results obtained in this study are the following:

The corrosion rate of the SAE 1020 steel with and without galvanization can vary depending on atmospheric pollutants.

Atmospheric corrosion promotes a loss of toughness by affecting the SAE 1020 steel, which can drop from 70 to 7 J.

Regarding the deterioration of the SAE 1020 steel when it is unprotected, the corrosion is markedly heterogeneous, and therefore toughness can vary drastically at one single location.

In comparison to the non-galvanized steel, the galvanized has a lower initial toughness, but it remains more constant over time, maintaining a range of 20 to 7 J.

ACKNOWLEDGEMENTS:
The authors gratefully acknowledge the support of the Chilean government through funds from the Innova-CORFO Project Nº 09CN14-5879 and the Department of Research at the *Pontificia Universidad Católica de Valparaíso*.

References

1. T. E. Graedel and C. Leygraf, *Atmospheric Corrosion*, Wiley-Interscience, New York (2000).
2. P. W. Brown and L.W. Masters, *Atmospheric Corrosion*, Wiley-Interscience, New York (1982).
3. I. L. Rozenfeld, *Atmospheric Corrosion of Metals*, NACE, Houston (1972).
4. K. Barton, *Protection against Atmospheric Corrosion*, Wiley, London (1976).
5. V. Kucera, E. Mattsson, *Corrosion Mechanisms*, Marcel Dekker, New York (1987).
6. J. M. Costa, M. Morcillo, S. Feliu, *Effect of environmental parameters on atmospheric corrosion of metals*, P.N. Cheremisinoff, Houston (1989).
7. Ph. Dillmann, F. Mazaudier, S. Hœrl, *Corros. Sci*. 46 (2004) 1401-1429.
8. H. Katayama, K. Noda, H. Masuda, M. Nagasawa, M. Itagaki, K. Watanabe, *Corros. Sci* 47 (2005) 2599-2606.
9. T. Kamimura, S. Hara, H. Miyuki, M. Yamashita, H. Uchida, *Corros. Sci* 48 (2006) 2799-2812.
10. A. Nazarov, D. Thierry, *Electrochim. Acta* 49 (2004) 2717-2724.
11. Y. Y. Chen, H. J. Tzeng, L. I. Wei, L. H. Wang, J. C. Oung, H. C. Shih, *Corros. Sci*. 47 (2005) 1001-1021.
12. R. Vera, D. Delgado, B. Rosales, *Corros. Sci*., 48(10) (2006) 2882-2900.
13. M. Okayasu, K. Sato, K. Okada, S. Yoshifuji, M. Mizuno, *J. Mater. Sci*. 44 (2009) 306-315.
14. S. Suresh, *Fatigue of Materials*, Cambridge University Press, New York (2004).
15. A. Ragab, H. Alawi, K. Sorein, *Mech. Mater*. 18 (1994) 69-77.
16. O. H. Ibrahim, *J. Mater. Sci. Technol*. 27 (2011) 931-936.
17. H. K. Sung, S.Y. Shin, B. Hwang, C. G. Lee, N. J. Kim, S. Lee, *Mater. Sci. Eng*., A 530 (2011) 530-538.
18. V. V. Kharchenko, E. A. Kondryakov, V. N. Zhmaka, A. A. Babutskii and A. Babutskii, *Strength Mater.* 38- 5 (2006) 535-541.
19. J. D. Verhoeven, *Steel Metallurgy for the Non-Metallurgist*, ASM International (2007).
20. R. Magnabosco and L. C. Rossetto, *J. Braz. Soc. Mech. Sci. & Eng*. 25(2) (2003).
21. ISO 9223, *Corrosion of metals and alloy-Classification of corrosivity of atmospheres*, ISO, Geneva (1991).
22. ISO 9224, *Corrosion of metals and alloys-Guiding values for the corrosivity categories of atmospheres*, ISO, Geneva (1991).
23. ISO 9225, *Corrosion of metals and Alloys-Corrosivity of atmospheres-methods of measurement of pollution*, ISO, Geneva (1991).
24. ISO 9226, *Corrosion of metals and alloys-Corrosivity of atmospheres-methods of determination corrosion rate of standard specimens for the evaluation of corrosivity*, ISO, Geneva (1991).
25. ASTM G50-10, *Standard Practice for Conducting Atmospheric Corrosion Tests on Metals.*
26. R. Vera, M. Puentes, R. Araya, P. Rojas, A. M. Carvajal, *Revista de la Construcción* 12(22) (2012) 61-72.
27. R. Vera, D. Delgado, R. Araya, M. Puentes, P. Rojas, I. Guerrero, G. Cabrera, S. Erazo, A. M. Carvajal, *Rev. LatinAm. Metal. Mat*. 32(2) (2012) 269-276.
28. R. Vera, B. M. Rosales, C. Tapia, *Corros. Sci.* 45 (2003) 321-337.